Inorganic Chemistry
Article

Inorg. Chem. **2009**, *48*, 7729–7739 **7729**
DOI: 10.1021/ic900527c

Oxidation of the Natural Amino Acids by a Ferryl Complex: Kinetic and Mechanistic Studies with Peptide Model Compounds

Ahmed I. Abouelatta, Ashley A. Campanali, Anil R. Ekkati, Mark Shamoun, Suneth Kalapugama, and Jeremy J. Kodanko*

Department of Chemistry, Wayne State University, 5101 Cass Ave, Detroit, Michigan 48202

Received March 18, 2009

Kinetic and mechanistic studies detailing the oxidation of substrates derived from the 20 natural amino acids by the ferryl complex $[Fe^{IV}(O)(N4Py)]^{2+}$ are described. Substrates of the general formula Ac-AA-NHtBu were treated with the ferryl complex under identical conditions ([Ac-AA-NHtBu] = 10 mM, [Fe] = 1 mM, 1:1 H_2O/CH_3CN), and pseudo-first-order rate constants were obtained. Relative rate constants calculated from these data illustrated the five most reactive substrates; in order of decreasing reactivity were those derived from Cys, Tyr, Trp, Met, and Gly. Second-order rate constants were determined for these substrates by varying substrate concentration under pseudo-first-order conditions. Substrates derived from the other natural amino acids did not display significant reactivity, accelerating decomposition of the ferryl complex at a rate less than 10 times that of the control reaction with no substrate added. Ferryl decomposition rates changed in D_2O/CD_3CN for the Cys, Tyr, and Trp substrates, giving deuterium kinetic isotope effects of 4.3, 29, and 5.2, respectively, consistent with electron-transfer, proton-transfer (Cys and Trp), or hydrogen atom abstraction (Tyr) mechanisms. Decomposition rates for $[Fe^{IV}(O)(N4Py)]^{2+}$ in the presence of the Met and Gly substrates were identical in H_2O/CH_3CN versus D_2O/CD_3CN solvents. A deuterium kinetic isotope effect of 4.8 was observed with the labeled substrate 2,2-d_2-Ac-Gly-NHtBu, consistent with $[Fe^{IV}(O)(N4Py)]^{2+}$ abstracting an α-hydrogen atom from Ac-Gly-NHtBu and generating a glycyl radical. Abstraction of α-hydrogen atoms from amino acid substrates other than Gly and oxidation of side chains contained in the amino acids other than Cys, Tyr, Trp, and Met were slow by comparison.

Introduction

Oxidized proteins accumulate during aging and in pathological conditions such as Alzheimer's disease. A consequence of oxidative stress, protein modification results from the chemical reactions of proteins with reactive oxygen species (ROS), including superoxide and the hydroxyl radical (·OH).[1] Due to the significance of protein oxidation in human health, studies regarding ROS damage have received considerable attention.[2−4] For instance, exposure of living cells to ionizing radiation[5] is known to elicit extensive damage to proteins by ·OH, an event which can trigger cell death. ROS species are known to damage proteins by several well-characterized mechanisms, including oxidation of amino acid side chains, backbone cleavage, or cross-link formation.[6] The exact nature of ROS damage to proteins depends on the oxidant, with powerful oxidants such as ·OH being the least selective and most destructive. Other oxidants such as $^1O_2$ or H_2O_2 are more selective, in some cases able to target single residues in proteins.[4]

Aside from playing detrimental roles in aging and various disease states, ROS have been used for practical applications, including the study of protein structure and protein targeting. Due to the fact that ·OH can affect scission of the protein backbone, metal complexes that generate ·OH, such as Fe^{II}(EDTA), are widely used during protein footprinting.[7] For footprinting applications, metal complexes can be anchored covalently to surface residues.[8] Alternatively, for targeting applications, noncovalent interactions can be used to localize the reagent at a specific binding site where it can affect cleavage. Examples include conjugates of protein affinity groups and EDTA for targeting calmodulin[9] and streptavidin,[10] as well as a Cu^{II}(phen) conjugate for targeting

*To whom correspondence should be addressed. E-mail: jkodanko@chem.wayne.edu.

(1) Swallow, A. J. *Radiation Chemistry of Organic Compounds*; Pergamon Press: Oxford, U. K., 1960.
(2) Garrison, W. M.; Jayko, M. E.; Bennett, W. *Radiat. Res.* **1962**, *16*, 483–502.
(3) Garrison, W. M. *Chem. Rev.* **1987**, *87*, 381–98.
(4) Davies, M. J. *Biochim. Biophys. Acta* **2005**, *1703*, 93–109.
(5) Schuessler, H.; Schilling, K. *Int. J. Radiat. Biol.* **1984**, *45*, 267–81.
(6) Berlett, B. S.; Stadtman, E. R. *J. Biol. Chem.* **1997**, *272*, 20313–20316.
(7) Zhong, M.; Lin, L.; Kallenbach, N. R. *Proc. Natl. Acad. Sci. U. S. A.* **1995**, *92*, 2111–15.
(8) Heyduk, T.; Baichoo, N.; Heyduk, E. *Met. Ions Biol. Syst.* **2001**, *38*, 255–287.
(9) Schepartz, A.; Cuenoud, B. *J. Am. Chem. Soc.* **1990**, *112*, 3247–9.
(10) Hoyer, D.; Cho, H.; Schultz, P. G. *J. Am. Chem. Soc.* **1990**, *112*, 3249–50.

Published on Web 07/13/2009

carbonic anhydrase.[11] In a similar manner, photosensitizers such as fluoroscein or malachite green, and recently the metal complex $Ru^{II}(bipy)_3$,[12] can be directed to a site on a protein and generate ROS upon photoexcitation. This process, known as chromophore-assisted light inactivation,[13−15] leads to oxidative damage within the direct vicinity of the photosensitizer, which can result in the inactivation of the target protein. In all of these cases, ROS are known to be "diffusible," that is, migrate from the locus point of the reagent to react with residues within a localized sphere of the generating reagent, where the radius of diffusion depends on the reactivity of the particular ROS.

Metal-based oxidants, where the reactive oxygen atom is bound to a metal center, represent an attractive alternative to ROS as reagents for protein oxidation, because they are nondiffusible and their reactivity can be tuned by controlling the nature of the ligand and metal. Surprisingly, metal-based oxidants have received much less attention than ROS in protein oxidation studies. One example of a reagent that generates a metal-based oxidant is the Ni^{II}-bound tripeptide Gly−Gly−His. When this complex was tethered to trifluoroperazine, site-specific cleavage of calmodulin was observed in the presence of the oxidant magnesium monoperoxypthalate.[16] Even though the identity of the metal-based oxidant was not established, this reaction occurred in the presence of catalase and was not affected by O_2, which is consistent with cleavage facilitated by a metal-based oxidant rather than by ROS. The same Ni-based reagent was also shown to cross-link proteins that are associated in solution.[17,18] In this case, cross-linking was not inhibited by hydroxyl radical scavengers, again consistent with the generation of a metal-based oxidant. Recently, the catalytic inactivation of carbonic anhydrase was accomplished with a sulfonamide derivative of the Cu^{II}-bound tripeptide Gly−Gly−His.[19] Although the nature of the oxidant was not established, oxidation of His and Trp side chains localized around the active site of the enzyme occurred, which is consistent with a nondiffusive oxidant being at play.

High-valent iron(IV)-oxo species, also known as ferryls, are metal-based oxidants that are involved in many biological oxidative transformations.[20,21] The key role of a ferryl species in the catalytic cycle of the heme iron enzyme cytochrome P450 is now widely accepted.[22] Ferryls have also been identified as intermediates in the catalytic cycles of the nonheme iron enzymes taurine:α-ketoglutarate dioxygenase[23] and the halogenase CytC3,[24] as well as the enzymes prolyl-4-hydroxylase[25] and tyrosine hydroxylase,[26] which oxidize amino acids. Although not detected directly, ferryls have been implicated as key intermediates in oxidation reactions catalyzed by phenylalanine and tryptophan hydroxylases.[21]

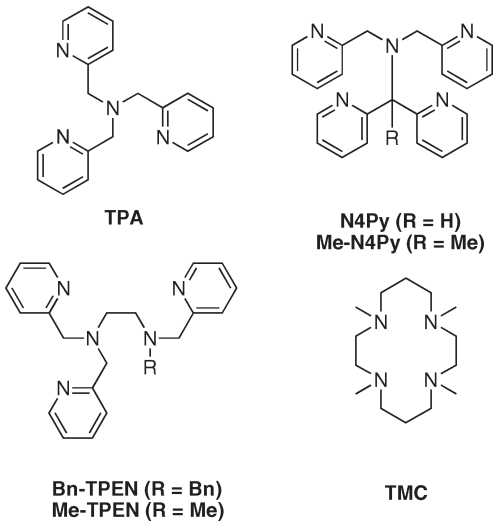

Figure 1. Nitrogen-rich heterocyclic ligands for constructing iron catalysts.

Significant progress has been made in the past decade regarding the generation of synthetic model complexes that mimic the oxidation chemistry of nonheme iron enzymes by generating metal-based oxidants.[20,27] Inspired by the metalloantibiotic bleomycin, which oxidizes DNA,[28−31] selective catalysts for hydrocarbon oxidation were discovered by moving away from carboxylate-rich ligand structures like EDTA, which is known to mediate the oxidation of hydrocarbons using ·OH (Fenton chemistry),[32−34] toward nitrogen-containing heterocycles as ligands (Figure 1). Examples include the tetradentate ligand TPA and its analogs, which catalyze the hydroxylation of a variety of hydrocarbon substrates using H_2O_2.[35−40] The large deuterium kinetic isotope effects (KIEs) observed with these reagents implicated iron-based oxidants as key intermediates that acted selectively, rather than radical chain autoxidation mechanisms involving ROS species. Later examples include ligands such

(11) Gallagher, J.; Zelenko, O.; Walts, A. D.; Sigman, D. S. *Biochemistry* **1998**, *37*, 2096–2104.
(12) Lee, J.; Yu, P.; Xiao, X.; Kodadek, T. *Mol. BioSyst.* **2008**, *4*, 59–65.
(13) Beck, S.; Sakurai, T.; Eustace, B. K.; Beste, G.; Schier, R.; Rudert, F.; Jay, D. G. *Proteomics* **2002**, *2*, 247–255.
(14) Jay, D. G. *Proc. Natl. Acad. Sci. U. S. A.* **1988**, *85*, 5454–8.
(15) Yan, P.; Xiong, Y.; Chen, B.; Negash, S.; Squier, T. C.; Mayer, M. U. *Biochemistry* **2006**, *45*, 4736–4748.
(16) Cuenoud, B.; Tarasow, T. M.; Schepartz, A. *Tetrahedron Lett.* **1992**, *33*, 895–898.
(17) Brown, K. C.; Yang, S.-H.; Kodadek, T. *Biochemistry* **1995**, *34*, 4733–4739.
(18) Brown, K. C.; Kodadek, T. *Met. Ions Biol. Syst.* **2001**, *38*, 351–384.
(19) Gokhale, N. H.; Cowan, J. A. *J. Biol. Inorg. Chem.* **2006**, *11*, 937–947.
(20) Nam, W. *Acc. Chem. Res.* **2007**, *40*, 522–531.
(21) Fitzpatrick, P. F. *Biochemistry* **2003**, *42*, 14083–14091.
(22) Denisov Ilia, G.; Makris Thomas, M.; Sligar Stephen, G.; Schlichting, I. *Chem. Rev.* **2005**, *105*, 2253–77.
(23) Price, J. C.; Barr, E. W.; Tirupati, B.; Bollinger, J. M.; Krebs, C. *Biochemistry* **2003**, *42*, 7497–7508.
(24) Galonic, D. P.; Barr, E. W.; Walsh, C. T.; Bollinger, J. M., Jr.; Krebs, C. *Nat. Chem. Biol.* **2006**, *3*, 113–116.
(25) Hoffart, L. M.; Barr, E. W.; Guyer, R. B.; Bollinger, J. M., Jr.; Krebs, C. *Proc. Natl. Acad. Sci. U. S. A.* **2006**, *103*, 14738–14743.
(26) Eser, B. E.; Barr, E. W.; Frantom, P. A.; Saleh, L.; Bollinger, J. M., Jr.; Krebs, C.; Fitzpatrick, P. F. *J. Am. Chem. Soc.* **2007**, *129*, 11334–11335.
(27) Que, L. *Acc. Chem. Res.* **2007**, *40*, 493–500.
(28) Hecht, S. M. *Anticancer Agents Nat. Prod.* **2005**, 357–381.
(29) Burger, R. M. *Chem. Rev.* **1998**, *98*, 1153–1169.
(30) Guajardo, R. J.; Hudson, S. E.; Brown, S. J.; Mascharak, P. K. *J. Am. Chem. Soc.* **1993**, *115*, 7971–7.
(31) Stubbe, J.; Kozarich, J. W. *Chem. Rev.* **1987**, *87*, 1107–36.
(32) Walling, C. *Acc. Chem. Res.* **1998**, *31*, 155–157.
(33) Fenton, H. J. H. *J. Chem. Soc., Trans.* **1894**, *65*, 899–910.
(34) Walling, C. *Acc. Chem. Res.* **1975**, *8*, 125–31.
(35) Rohde, J.-U.; Stubna, A.; Bominaar, E. L.; Muenck, E.; Nam, W.; Que, L., Jr. *Inorg. Chem.* **2006**, *45*, 6435–6445.
(36) Britovsek, G. J. P.; England, J.; White, A. J. P. *Inorg. Chem.* **2005**, *44*, 8125–8134.
(37) Kaizer, J.; Klinker, E. J.; Oh, N. Y.; Rohde, J.-U.; Song, W. J.; Stubna, A.; Kim, J.; Muenck, E.; Nam, W.; Que, L., Jr. *J. Am. Chem. Soc.* **2004**, *126*, 472–473.
(38) Lim, M. H.; Rohde, J.-U.; Stubna, A.; Bukowski, M. R.; Costas, M.; Ho, R. Y. N.; Munck, E.; Nam, W.; Que, L., Jr. *Proc. Natl. Acad. Sci. U. S. A.* **2003**, *100*, 3665–3670.
(39) Chen, K.; Que, L., Jr. *J. Am. Chem. Soc.* **2001**, *123*, 6327–6337.
(40) Kim, J.; Harrison, R. G.; Kim, C.; Que, L., Jr. *J. Am. Chem. Soc.* **1996**, *118*, 4373–9.

as TMC (1,4,8,11-tetramethyl-1,4,8,11-tetraazacyclotetradecane), N4Py (*N*,*N*-bis(2-pyridylmethyl)-*N*-bis(2-pyridyl)-methylamine), and Bn-TPEN (*N*-benzyl-*N*,*N*′,*N*′-tris(2-pyridylmethyl)ethane-1,2-diamine), which generate well-characterized ferryl species[41,42] with remarkable reactivity, capable of oxidizing strong C−H bonds with bond dissociation energies as high as 99 kcal/mol with high kinetic selectivity and KIEs as high as 50.[37,43,44] Ferryls derived from pentadentate ligands can be highly stable in the absence of a substrate. For instance, the ferryl species $[Fe^{IV}(O)(N4Py)]^{2+}$ was found to be stable in aqueous solutions for several days at room temperature.[45] Besides simple hydrocarbons,[46−48] more recent work has demonstrated that ferryls such as $[Fe^{IV}(O)(N4Py)]^{2+}$ oxidize aromatics,[49,50] sulfides,[45] anilines,[51,52] alcohols,[53] catechols,[54] and NADH analogs.[55] In addition to the oxidation of small molecules, ferrous complexes based on the ligands N4Py and Me-TPEN cleave DNA in the presence of O_2,[56−58] which illustrates their potential to oxidize biomolecules.

Considering this background, our research aim was to explore the reactivity of a well-characterized iron-based oxidant with amino acids and to determine whether backbone cleavage or side-chain oxidation would occur. For these studies, we constructed a series of protected amino acid substrates (Ac-AA-NHtBu) from the 20 natural amino acids that were designed to mimic individual residues within a polypeptide chain. These substrates were subjected to oxidation using the ferryl species $[Fe^{IV}(O)(N4Py)]^{2+}$.[42,45] Preliminary data in this area were reported previously by our group.[59] Herein, we report a comprehensive study of reactivity and reaction mechanism with the 20 natural amino acids.

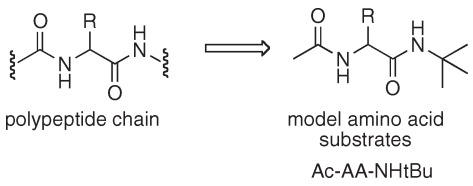

Figure 2. Model amino acid substrates.

Results and Discussion

Kinetic Studies. To begin studies in this area, we established how rapidly a ferryl species reacts with each of the 20 amino acids. A series of protected amino acid substrates was constructed from the 20 natural amino acids that were designed to model individual residues within a polypeptide chain (Figure 2). In the model substrates, the *N*-termini were acetylated, and *tert*-butyl amides were installed to block the weak C−H bonds that would be equivalent to the α position of the next residue in a polypeptide chain. The purpose of these studies was to establish quantitatively the relative rates of reaction for the amino acid substrates with a ferryl complex. We chose to measure rates of reaction for natural amino acids with the ferryl species $[Fe^{IV}(O)(N4Py)]^{2+}$, which is a well-characterized iron-based oxidant with an absorbance band in the visible region (λ_{max} = 680 nm). For these experiments, the iron-based oxidant $[Fe^{IV}(O)(N4Py)]^{2+}$ was pregenerated ([Fe] = 1 mM, 1:1 H_2O/CH_3CN) with $KHSO_5$[45] and treated with 10 equiv of the substrate, and decomposition of the ferryl was measured over time (Figure S1, Supporting Information). Pseudo-first-order (k_{obs}) and relative rate constants (k_{rel}; Table 1) were derived that indicated the kinetic order of reactivity for amino acids. These experiments established that the Cys and Tyr substrates promote decomposition of the ferryl species most rapidly ($t_{1/2} < 5$ s), followed by Trp and Met. The Gly, His, and Ser derivatives were of intermediate reactivity. All other substrates caused decomposition of $[Fe^{IV}(O)(N4Py)]^{2+}$ at a slower rate, at least three times slower than that of Gly and close to the background decomposition rate of $[Fe^{IV}(O)(N4Py)]^{2+}$ with no substrate added, indicating that these amino acids were slow to react with the iron-based oxidant, if they reacted at all. The broad range of k_{rel} values shown in Table 1, which vary by over 5 orders of magnitude, illustrates that $[Fe^{IV}(O)(N4Py)]^{2+}$ has the potential to be more selective than ·OH, whose kinetic rate constants vary by only 3 orders of magnitude in reactions with amino acids.[60]

Mechanistic Studies. After compiling the kinetic data in Table 1, mechanistic studies were carried out with reactive substrates in order to determine each mode of reactivity. Substrates derived from Cys, Tyr, Trp, Met, and Gly were considered for these studies, because the decomposition rates for $[Fe^{IV}(O)(N4Py)]^{2+}$ were greater than 10 times that of the control experiment with no substrate added; thus, they were significant from a kinetic standpoint. Substrates were evaluated using two general

(41) Rohde, J.-U.; In, J.-H.; Lim, M. H.; Brennessel, W. W.; Bukowski, M. R.; Stubna, A.; Münck, E.; Nam, W.; Que, L. *Science* **2003**, *299*, 1037–1039.
(42) Klinker, E. J.; Kaizer, J.; Brennessel, W. W.; Woodrum, N. L.; Cramer, C. J.; Que, L., Jr. *Angew. Chem., Int. Ed.* **2005**, *44*, 3690–3694.
(43) de Visser, S. P.; Oh, K.; Han, A.-R.; Nam, W. *Inorg. Chem.* **2007**, *46*, 4632–4641.
(44) van den Berg, T. A.; de Boer, J. W.; Browne, W. R.; Roelfes, G.; Feringa, B. L. *Chem. Commun.* **2004**, 2550–2551.
(45) Sastri, C. V.; Seo, M. S.; Park, M. J.; Kim, K. M.; Nam, W. *Chem. Commun.* **2005**, 1405–1407.
(46) van den Berg, T. A.; de Boer, J. W.; Browne, W. R.; Roelfes, G.; Feringa, B. L. *Chem. Commun.* **2004**, 2550–2551.
(47) Kaizer, J.; Klinker, E. J.; Oh, N. Y.; Rohde, J.-U.; Song, W. J.; Stubna, A.; Kim, J.; Münck, E.; Nam, W.; Que, L., Jr. *J. Am. Chem. Soc.* **2004**, *126*, 472–473.
(48) Roelfes, G.; Lubben, M.; Hage, R.; Que, L., Jr.; Feringa, B. L. *Chem.—Eur. J.* **2000**, *6*, 2152–2159.
(49) Kang, M.-J.; Song, W. J.; Han, A.-R.; Choi, Y. S.; Jang, H. G.; Nam, W. *J. Org. Chem.* **2007**, *72*, 6301–6304.
(50) de Visser, S. P.; Oh, K.; Han, A.-R.; Nam, W. *Inorg. Chem.* **2007**, *46*, 4632–4641.
(51) Nehru, K.; Seo, M. S.; Kim, J.; Nam, W. *Inorg. Chem.* **2007**, *46*, 293–298.
(52) Nehru, K.; Jang, Y. K.; Seo, M. S.; Nam, W.; Kim, J. *Bull. Korean Chem. Soc.* **2007**, *28*, 843–846.
(53) Oh, N. Y.; Suh, Y.; Park, M. J.; Seo, M. S.; Kim, J.; Nam, W. *Angew. Chem., Int. Ed.* **2005**, *44*, 4235–4239.
(54) Nehru, K.; Jang, Y.; Oh, S.; Dallemer, F.; Nam, W.; Kim, J. *Inorg. Chim. Acta* **2008**, *361*, 2557–2561.
(55) Fukuzumi, S.; Kotani, H.; Lee, Y.-M.; Nam, W. *J. Am. Chem. Soc.* **2008**, *130*, 15134–15142.
(56) van den Berg, T. A.; Feringa, B. L.; Roelfes, G. *Chem. Commun.* **2007**, 180–182.
(57) Roelfes, G.; Branum, M. E.; Wang, L.; Que, L., Jr.; Feringa, B. L. *J. Am. Chem. Soc.* **2000**, *122*, 11517–11518.
(58) Mialane, P.; Nivorojkine, A.; Pratviel, G.; Azema, L.; Slany, M.; Godde, F.; Simaan, A.; Banse, F.; Kargar-Grisel, T.; Bouchoux, G.; Sainton, J.; Horner, O.; Guilhem, J.; Tchertanova, L.; Meunier, B.; Girerd, J.-J. *Inorg. Chem.* **1999**, *38*, 1085–1092.
(59) Ekkati, A. R.; Kodanko, J. J. *J. Am. Chem. Soc.* **2007**, *129*, 12390–12391.
(60) Buxton, G. V.; Greenstock, C. L.; Helman, W. P.; Ross, A. B. *J. Phys. Chem. Ref. Data* **1988**, *17*, 513–886.

Table 1. Pseudo-First-Order Rate Constants for Decomposition of $[Fe^{IV}(O)(N4Py)]^{2+}$ by Amino Acid Substrates Ac-AA-NHtBu ([Fe] = 1 mM)[a,b]

entry	Ac-AA-NHtBu	k_{obs} (s^{-1})[c]	k_{rel}
1	Cys	1.7(1)	340000
2	Tyr	$3.4(1) \times 10^{-1}$	68000
3	Trp	$1.7(1) \times 10^{-2}$	3400
4	Met	$3.2(1) \times 10^{-3}$	640
5	Gly	$5.8(2) \times 10^{-5}$	12
6	His	$3.8(2) \times 10^{-5}$	7.6
7	Ser	$3.3(7) \times 10^{-5}$	6.6
8	Ala	$2.5(2) \times 10^{-5}$	5.0
9	Asp	$1.7(3) \times 10^{-5}$	3.4
10	Gln	$1.6(2) \times 10^{-5}$	3.2
11	Thr	$1.4(6) \times 10^{-5}$	2.8
12	Phe	$1.4(4) \times 10^{-5}$	2.8
13	Asn	$1.4(1) \times 10^{-5}$	2.8
14	Arg·HCl[d]	$1.4(1) \times 10^{-5}$	2.8
15	Lys·HCl[d]	$1.4(2) \times 10^{-5}$	2.8
16	Glu	$1.3(1) \times 10^{-5}$	2.6
17	Val	$1.3(2) \times 10^{-5}$	2.6
18	Leu	$7.4(3) \times 10^{-6}$	1.5
19	Pro	$5.0(8) \times 10^{-6}$	1.0
20	Ile	$5.0(5) \times 10^{-6}$	1.0

[a] Reaction conditions: 1:1 H_2O/CH_3CN, 298 ± 2 K, 10 mM substrate (10 equiv). [b] Background rate for decomposition of $[Fe^{IV}(O)(N4Py)]^{2+}$ in the absence of a substrate was $5.0(2) \times 10^{-6}$ s^{-1}. [c] Number reported is the average of at least three runs; error as standard deviation is given in parentheses. [d] HCl salts of the basic amino acids were used to avoid strongly basic conditions, see text for details.

protocols. The first protocol involved gathering kinetic data under pseudo-first-order conditions with 10 equiv of Ac-AA-NHtBu compared to $[Fe^{IV}(O)(N4Py)]^{2+}$. Subsequently, second-order rate constants were determined by varying the concentration of the substrate under pseudo-first-order conditions. In some cases, catalytic reactions were performed with stoichiometric $KHSO_5$ and a catalytic amount of $[Fe^{II}(CH_3CN)(N4Py)](ClO_4)_2$, as reported previously.[59] However, these catalytic conditions were used sparingly, due to a fast background reaction of some substrates with $KHSO_5$ in the absence of an iron catalyst.

Reactive Amino Acids. Cysteine. The fastest reacting substrate was derived from Cys, which caused decomposition of $[Fe^{IV}(O)(N4Py)]^{2+}$ at a rate over 5 orders of magnitude faster than the control reaction with no substrate added (Table 1). A second-order rate constant of $1.9(3) \times 10^2$ M^{-1} s^{-1} was determined by plotting pseudo-first-order rate constants (k_{obs}) versus the concentration of Ac-Cys-NHtBu (Figure 3a). In order to gain insight into the mechanism of the reaction of Ac-Cys-NHtBu with $[Fe^{IV}(O)(N4Py)]^{2+}$ (Scheme 1), the same reaction was performed in a 1:1 mixture of the deuterated solvents D_2O/CD_3CN. In this solvent mixture, the sulfide and amide protons of Ac-Cys-NHtBu exchange readily to form the labeled substrate with three deuterium atoms incorporated (confirmed by ^1H NMR spectroscopy). The rate of decomposition for $[Fe^{IV}(O)(N4Py)]^{2+}$ in D_2O/CD_3CN was determined to be $3.7(1) \times 10^{-1}$ s^{-1}, which is substantially slower than the same reaction in the H_2O/CH_3CN solvent, and gives a deuterium kinetic isotope effect (k_H/k_D) of 4.3 (Figure 3b). The possibility that the KIE was due to a solvent effect was negated by the fact that some substrates do not show KIEs in the D_2O/CD_3CN solvent (vide infra). This KIE is consistent with a rate-limiting electron-transfer, followed by a proton-transfer (ET-PT), to form the thiyl radical and $[Fe^{III}(OH)(N4Py)]^{2+}$, rather

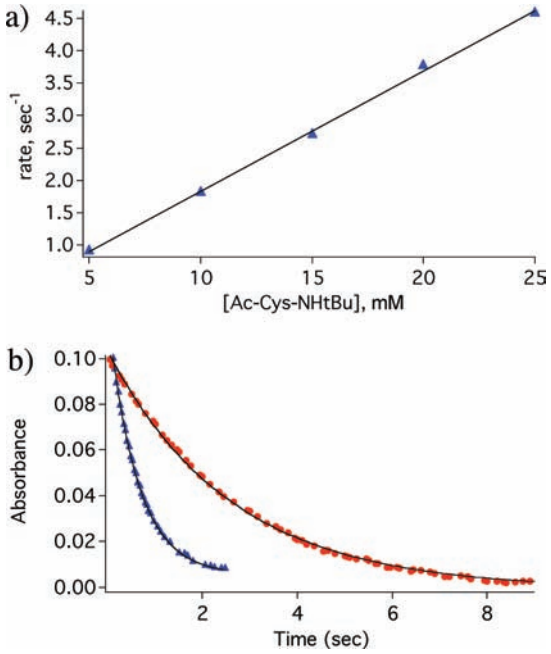

Figure 3. (a) Plot of pseudo-first-order rate constants (k_{obs}) against the concentration of Ac-Cys-NHtBu to determine the second-order rate constant at 298 ± 2 K. (b) Time course of the decay of $[Fe^{IV}(O)(N4Py)]^{2+}$ (1 mM) upon treatment with Ac-Cys-NHtBu (10 equiv) in 1:1 H_2O/CH_3CN (absorbance at 680 nm = ▲, blue; calculated fit = black line) vs 1:1 D_2O/CD_3CN (absorbance at 680 nm = ●●, red; calculated fit = black line) at 298 ± 2 K.

Scheme 1. Proposed Mechanism for Reaction of $[Fe^{IV}(O)(N4Py)]^{2+}$ with Ac-Cys-NHtBu

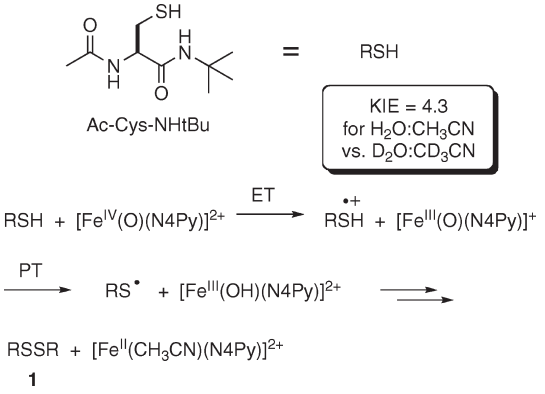

than a concerted hydrogen atom transfer (HAT), where a much larger KIE would be expected.[51,61] The regeneration of $[Fe^{II}(CH_3CN)(N4Py)]^{2+}$ was considerably slower than the decomposition of $[Fe^{IV}(O)(N4Py)]^{2+}$, consistent with the formation of a long-lived $[Fe^{III}(OH)(N4Py)]^{2+}$ species. A facile electron transfer from Ac-Cys-NHtBu to $[Fe^{IV}(O)(N4Py)]^{2+}$ is not surprising, given the high $E_{1/2}$ value (+0.9 V)[62] for the $Fe^{III/IV}$ couple of $[Fe^{IV}(O)(N4Py)]^{2+}$ and the reducing power of thiols.[63] Product analysis revealed that disulfide **1** was formed as the final product

(61) A mechanism involving HAT cannot be ruled out on the basis of the KIE value alone.

(62) Collins, M. J.; Ray, K.; Que, L., Jr. *Inorg. Chem.* **2006**, *45*, 8009–8011.

(63) A note of caution was added because a lower $E_{1/2}$ value of +0.5 V was determined for $[Fe^{IV}(O)(N4Py)]^{2+}$ in a later publication. See: Lee, Y.-M.; Kotani, H.; Suenobu, T.; Nam, W.; Fukuzumi, S. *J. Am. Chem. Soc.* **2008**, *130*, 434–435.

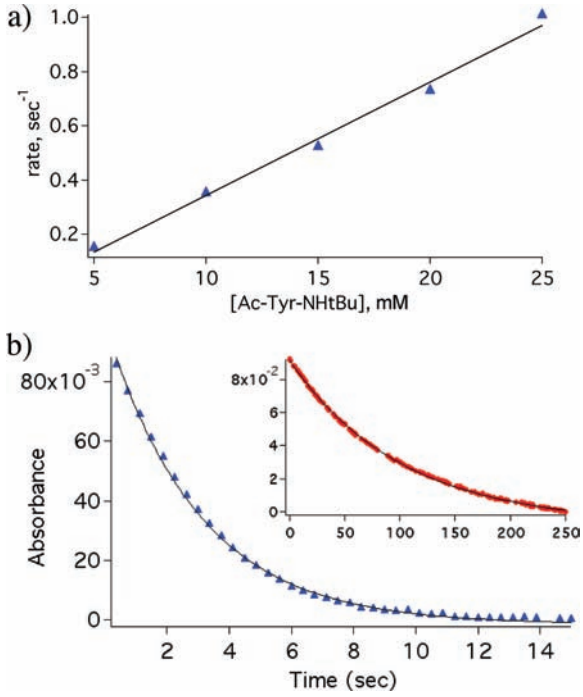

Figure 4. (a) Plot of pseudo-first-order rate constants (k_{obs}) against the concentration of Ac-Tyr-NHtBu to determine the second-order rate constant at 298 ± 2 K. (b) Time course of the decay of $[Fe^{IV}(O)(N4Py)]^{2+}$ (1 mM) upon treatment with Ac-Tyr-NHtBu (10 equiv) in 1:1 H_2O/CH_3CN (absorbance at 680 nm = ▲, blue; calculated fit = black line). Inset: 1:1 D_2O/CD_3CN (absorbance at 680 nm = ●●, red; calculated fit = black line) at 298 ± 2 K.

from the reaction in 61% yield based on $[Fe^{IV}(O)(N4Py)]^{2+}$ under pseudo-first-order conditions. Other oxidized products, such as sulfenic or sulfinic acids derived from the Cys substrate, were not detected.

Tyrosine. The substrate Ac-Tyr-NHtBu was the second most reactive, causing decomposition of $[Fe^{IV}(O)(N4Py)]^{2+}$ at a rate that is over 4 orders of magnitude faster than that of the control reaction. For the Tyr substrate, a second-order rate constant of $4.2(3) \times 10^1$ M^{-1} s^{-1} was determined (Figure 4a). A primary KIE of 29 was observed for decomposition of $[Fe^{IV}(O)(N4Py)]^{2+}$ by Ac-Tyr-NHtBu in D_2O/CD_3CN compared to H_2O/CH_3CN solvent, which is consistent with a HAT mechanism and the generation of a tyrosyl radical, rather than ET-PT (Figure 4b).[51] This hypothesis is consistent with the slower rate constant measured for the decomposition of $[Fe^{IV}(O)(N4Py)]^{2+}$ in the presence of the protected Tyr derivative Ac-Tyr(OAc)-NHtBu (Scheme 2), which was determined to be $1.3(2) \times 10^{-5}$ s^{-1}, >26 000 times slower than the rate of decomposition with Ac-Tyr-NHtBu. Similarly, a rate constant of $2.5(2) \times 10^{-5}$ s^{-1} was measured for the reaction of Ac-Tyr(OMe)-NHtBu and $[Fe^{IV}(O)(N4Py)]^{2+}$, which was >13 000 times slower. Both rates were similar to the decomposition rate observed with Ac-Phe-NHtBu (entry 12, Table 1). Therefore, the hydroxyl functional group of Ac-Tyr-NHtBu, rather than the electron-rich aromatic ring, is directly responsible for the high reactivity observed. Only a trace amount of the phenoxyl radical derived from Ac-Tyr-NHtBu was detected by electron paramagnetic resonance (EPR) spectroscopy (Figure S24, Supporting Information), presumably due to its instability. However,

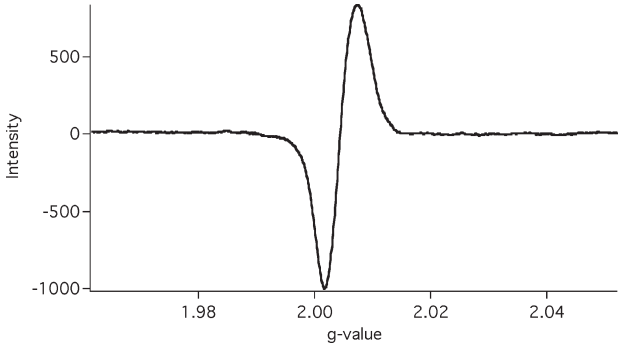

Figure 5. X-band EPR spectrum of phenoxyl radical generated from the reaction of 2,4,6-tri-*tert*-butylphenol and $[Fe^{IV}(O)(N4Py)]^{2+}$ in H_2O/CH_3CN. Experimental conditions: temperature, 125 K; microwaves, 1.1 mW at 9.34 GHz; modulation, 0.55 G; receiver gain, 100.

Scheme 2. Proposed Mechanism for the Reaction of $[Fe^{IV}(O)(N4Py)]^{2+}$ with Ac-Tyr-NHtBu

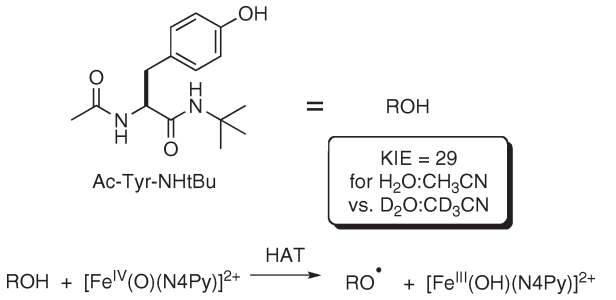

the more stable phenoxyl radical derived from 2,4,6-tri-*tert*-butylphenol was observed by EPR (signal at g = 2.0045) upon treating this phenol with $[Fe^{IV}(O)(N4Py)]^{2+}$ under the same conditions (Figure 5). Decomposition of the Ac-Tyr-NHtBu substrate was observed from the reaction with $[Fe^{IV}(O)(N4Py)]^{2+}$, and no major products were identified, presumably due to the propensity of phenoxyl radicals to polymerize.

Tryptophan. The substrate derived from tryptophan was the third most reactive, decomposing $[Fe^{IV}(O)(N4Py)]^{2+}$ more than 3 orders of magnitude faster than the control reaction. For the Trp substrate, a second-order rate constant of 1.6(4) M^{-1} s^{-1} was determined (Figure 6a). A KIE of 5.2 was observed for the decomposition of $[Fe^{IV}(O)(N4Py)]^{2+}$ by Ac-Trp-NHtBu in D_2O/CD_3CN ($k_{obs} = 3.3(1) \times 10^{-3}$ s^{-1}) compared to that in the H_2O/CH_3CN solvent (Figure 6b). In these experiments, full deuterium exchange of all three acidic protons of the substrate Ac-Trp-NHtBu was complete after 2 days according to ^1H NMR analysis. The magnitude of this isotope effect is most consistent with an ET-PT mechanism (Scheme 3)[61] and is similar to the KIE of 4.4 measured for the oxidation of tryptophan in D_2O by the heme-containing iron enzyme tryptophan 2,3-dioxygenase, where removal of the indole proton was proposed to be at least partially rate-determining.[64] It was noted in the oxidation reaction with the Trp substrate that decomposition of $[Fe^{IV}(O)(N4Py)]^{2+}$ (λ_{max} = 680 nm) was much faster than regeneration of $[Fe^{II}(CH_3CN)(N4Py)]^{2+}$ (λ_{max} = 450 nm) according to UV−vis spectroscopy (Figure 7), which is

(64) Leeds, J. M.; Brown, P. J.; McGeehan, G. M.; Brown, F. K.; Wiseman, J. S. *J. Biol. Chem.* **1993**, *268*, 17781–6.

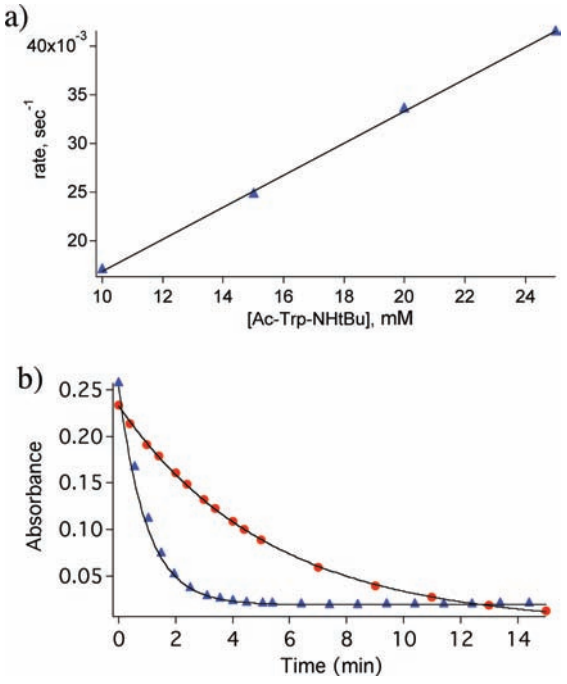

Figure 6. (a) Plot of pseudo-first-order rate constants (k_{obs}) against the concentration of Ac-Trp-NHtBu to determine the second-order rate constant at 298 ± 2 K. (b) Time course of the decay of $[Fe^{IV}(O)(N4Py)]^{2+}$ (1 mM) upon treatment with Ac-Trp-NHtBu (10 equiv) in 1:1 H_2O/CH_3CN (absorbance at 680 nm = ▲▲, blue; calculated fit = black line) vs 1:1 D_2O/CD_3CN (absorbance at 680 nm = ● ●, red; calculated fit = black line) at 298 ± 2 K.

consistent with the presence of a long-lived Fe^{III} intermediate, most likely $[Fe^{III}(OH)(N4Py)]^{2+}$. In this case, radical rebound between $[Fe^{III}(OH)(N4Py)]^{2+}$ and the tryptophan radical would be slow. Consistent with this idea, a trace amount of the organic radical was detected by EPR spectroscopy immediately after the addition of Ac-Trp-NHtBu to $[Fe^{IV}(O)(N4Py)]^{2+}$ (Figure S25, Supporting Information). Products consistent with the addition of a single oxygen atom to the Trp substrate, most likely at the 3 position of the indole ring,[65] were identified by electrospray mass spectrometry (ESMS) analysis (M + H = 318) of the crude reaction mixture. However, the isolation and full characterization of these products was hampered by the complexity of the mixture.[66]

Methionine. The substrate Ac-Met-NHtBu was the fourth most reactive, causing decomposition of $[Fe^{IV}(O)(N4Py)]^{2+}$ to occur 640 times faster than the control reaction. A second-order rate constant of $3.2(4) \times 10^{-1}$ M^{-1} s^{-1} was determined for the Met substrate (Figure 8a). Rates for the decomposition of $[Fe^{IV}(O)(N4Py)]^{2+}$ were identical within error in D_2O/CD_3CN (k_{obs} = $3.0(2) \times 10^{-3}$ s^{-1}) compared to those in the H_2O/CH_3CN solvent, indicating that the loss of a proton did not occur during the rate-limiting step (Figure 8b). The fact that no KIE was observed is consistent with the solvent effect being negligible for the oxidations by $[Fe^{IV}(O)(N4Py)]^{2+}$ in D_2O/CD_3CN, which supports the hypothesis that the loss of a proton or hydrogen atom

(65) Stewart, D. J.; Napolitano, M. J.; Bakhmutova-Albert, E. V.; Margerum, D. W. *Inorg. Chem.* **2008**, *47*, 1639–1647.

(66) The acyl lactam product noted in ref 59 was not observed in this kinetic experiment because excess $KHSO_5$ was not added.

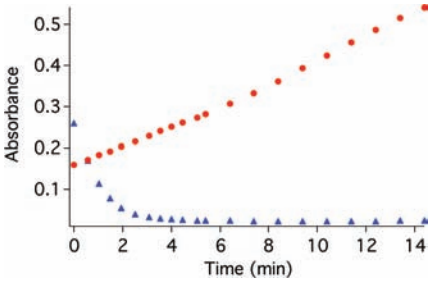

Figure 7. Time course for the decomposition of $[Fe^{IV}(O)(N4Py)]^{2+}$ (λ_{max} = 680 nm, ▲▲, blue) and delayed regeneration of $[Fe^{II}(CH_3CN)(N4Py)]^{2+}$ (λ_{max} = 450 nm, ● ●, red) during reaction of Ac-Trp-NHtBu with $[Fe^{IV}(O)(N4Py)]^{2+}$ in 1:1 H_2O/CH_3CN under pseudo-first-order conditions.

Scheme 3. Proposed Mechanism for Reaction of $[Fe^{IV}(O)(N4Py)]^{2+}$ with Ac-Trp-NHtBu

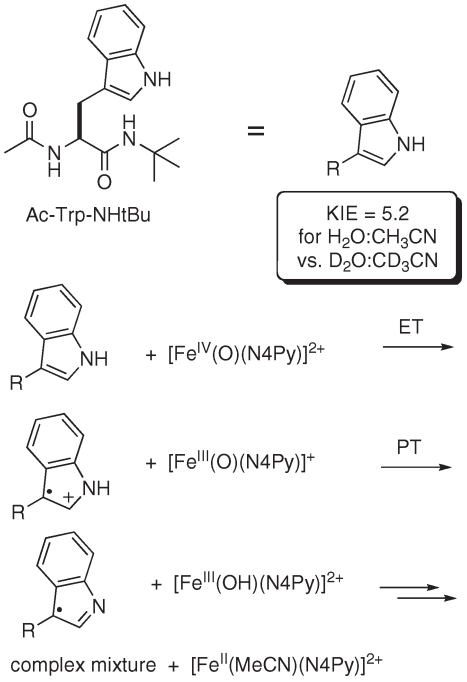

from the substrate was responsible for generating the KIEs measured with the Cys, Tyr, and Trp substrates. When the same reaction was conducted using equimolar amounts of $[Fe^{IV}(O)(N4Py)]^{2+}$ and Ac-Met-NHtBu (1 mM each), a mixture of two diastereomeric sulfoxides was formed in 31% yield, along with 54% recovered starting material. Under these single turnover conditions, no sulfone product was detected by NMR or ESMS analysis of the crude reaction mixture, indicating that the first oxidation of sulfide to sulfoxide occurs at a faster rate than the subsequent oxidation of sulfoxide to sulfone, consistent with previous studies.[45] Therefore, the oxidation of Ac-Met-NHtBu to the sulfone product observed under catalytic conditions with stoichiometric $KHSO_5$ was due to the background reaction of $KHSO_5$ with the sulfide, in the absence of an iron catalyst, as previously described.[59] Taken together, these data are consistent with an oxygen-atom transfer reaction occurring between the $[Fe^{IV}(O)(N4Py)]^{2+}$ and the Ac-Met-NHtBu substrate to yield sulfoxide product **2** (Scheme 4). Furthermore, the rate constant obtained for

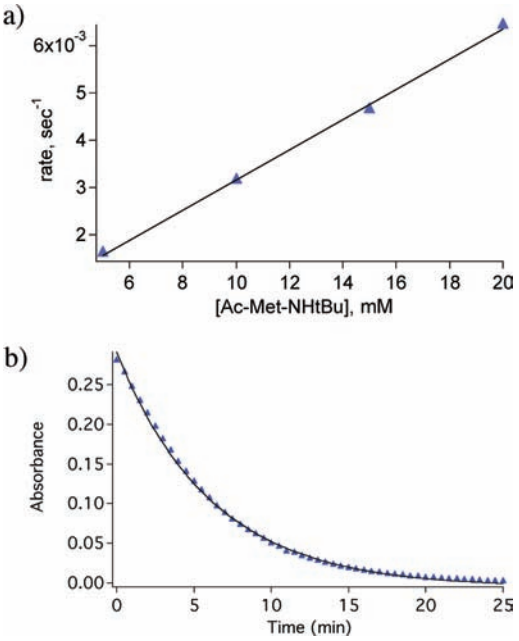

Figure 8. (a) Plot of pseudo-first-order rate constants (k_{obs}) against the concentration of Ac-Met-NHtBu to determine the second-order rate constant at 298 ± 2 K. (b) Time course of the decay of $[Fe^{IV}(O)(N4Py)]^{2+}$ (1 mM) upon treatment with Ac-Met-NHtBu (10 equiv) in 1:1 D_2O/CD_3CN (absorbance at 680 nm = ▲, blue; calculated fit = black line) at 298 ± 2 K.

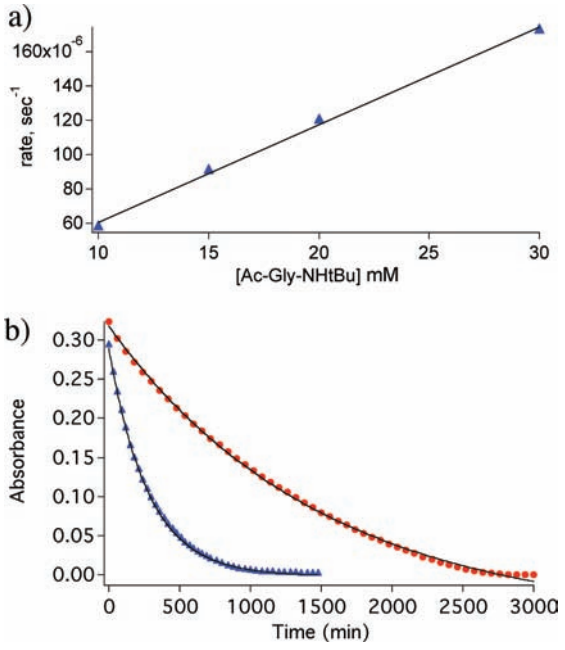

Figure 9. (a) Plot of pseudo-first-order rate constants (k_{obs}) against the concentration of Ac-Gly-NHtBu to determine the second-order rate constant at 298 ± 2 K. (b) Time course of the decay of $[Fe^{IV}(O)(N4Py)]^{2+}$ (1 mM) upon treatment with Ac-Gly-NHtBu (10 equiv) in 1:1 H_2O/CH_3CN (absorbance at 680 nm = ▲, blue; calculated fit = black line) vs treatment with 2,2-d_2-Ac-Gly-NHtBu (10 equiv) in 1:1 H_2O/CH_3CN (absorbance at 680 nm = ● ●, red; calculated fit = black line) at 298 ± 2 K.

Ac-Met-NHtBu agrees well with previous data from reactivity studies of $[Fe^{IV}(O)(N4Py)]^{2+}$ with aromatic sulfides.[45]

Glycine. The substrate derived from Gly ranked fifth in overall reactivity with $[Fe^{IV}(O)(N4Py)]^{2+}$, causing decomposition of the ferryl to occur 12 times faster than the control reaction. A second-order rate constant of $5.7(7) \times 10^{-3}$ M^{-1} s^{-1} was determined for the Gly substrate (Figure 9a). As observed with the Met substrate, decomposition of $[Fe^{IV}(O)(N4Py)]^{2+}$ occurred at an identical rate, within error, in D_2O/CD_3CN (k_{obs} = $6.1(1) \times 10^{-5}$ s^{-1}), indicating that deprotonation of an amide proton of Ac-Gly-NHtBu was not involved in the rate-determining step of ferryl decomposition. In contrast, when the Gly substrate was labeled with deuterium at the α position (2,2-d_2), decomposition of $[Fe^{IV}(O)(N4Py)]^{2+}$ was much slower with $k_{obs} = 1.2(5) \times 10^{-5}$ s^{-1} (KIE = 4.8; Figure 9b), which is consistent with the ferryl species generating a glycyl radical (Scheme 5).[61]

Interestingly, product analysis indicated that no major products derived from Ac-Gly-NHtBu were formed in the reaction of $[Fe^{IV}(O)(N4Py)]^{2+}$ with this substrate under single-turnover conditions, and only starting material was recovered. However, it was noted that the N4Py ligand was converted into di(2-pyridyl)ketone (**4**). Considering the fact that the Gly substrate clearly accelerates the decomposition of $[Fe^{IV}(O)(N4Py)]^{2+}$, there was a primary KIE observed, and yet there was no product derived from Ac-Gly-NHtBu detected, the following mechanistic scheme is proposed for the single-turnover experiment (Figure 10a). Reaction of $[Fe^{IV}(O)(N4Py)]^{2+}$ with Ac-Gly-NHtBu results in the formation of a glycyl radical intermediate. Subsequent oxidation of the N4Py ligand by this radical intermediate results in the hydroxylation of the ligand forming **3**, which breaks down into **4**. This mechanistic hypothesis is supported by

Scheme 4. Proposed Mechanism for Reaction of $[Fe^{IV}(O)(N4Py)]^{2+}$ with Ac-Met-NHtBu

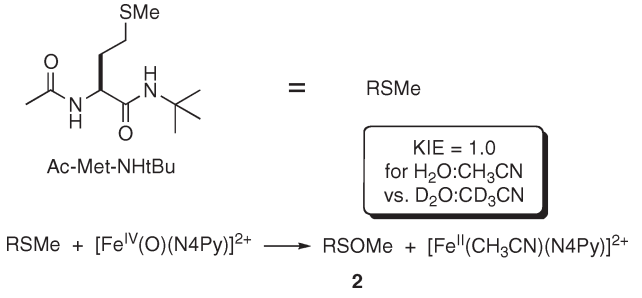

Scheme 5. Proposed Mechanism for Reaction of $[Fe^{IV}(O)(N4Py)]^{2+}$ with Ac-Gly-NHtBu

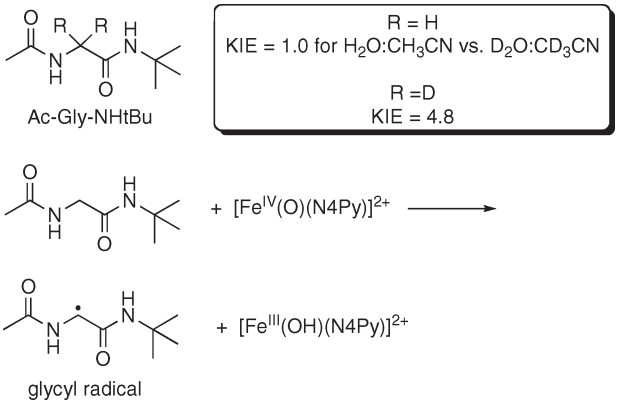

the fact that oxidized Gly products are observed from the single-turnover experiment of Ac-Gly-NHtBu with the ferryl $[Fe^{IV}(O)(Me\text{-}N4Py)]^{2+}$ (see Figure 1), which does

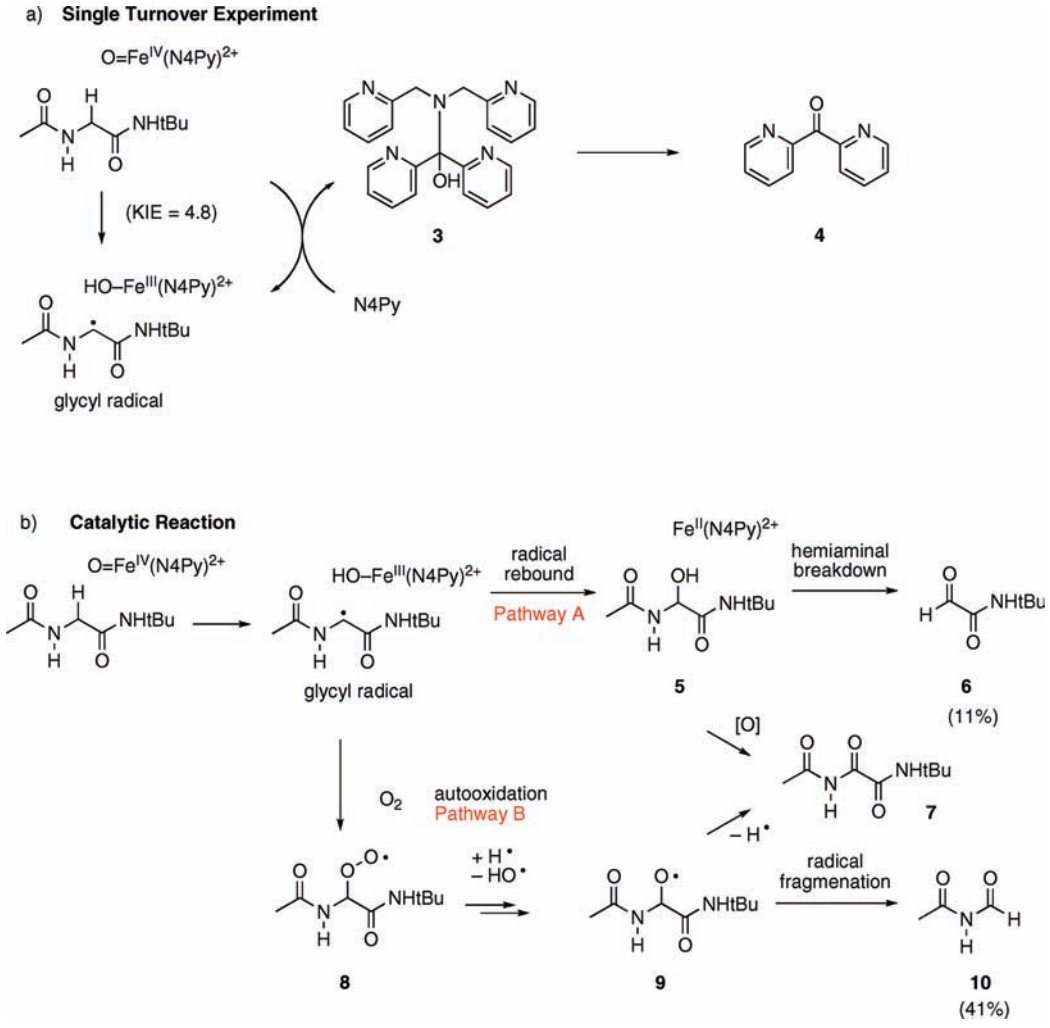

Figure 10. Proposed mechanism for the oxidation of Ac-Gly-NHtBu under single-turnover (a) and catalytic (b) conditions.

not possess the same weak C−H bond as N4Py. The fact that no products are formed under single-turnover conditions signifies that radical rebound between $[Fe^{III}(OH)(N4Py)]^{2+}$ and the glycyl radical is slow. The H-atom "shuffle" between the Gly substrate and the N4Py ligand shown in Figure 10a is strikingly similar to the role of glycyl radicals in proteins, which act as transient intermediates that shuttle radicals from one center to another.[67]

Results from the single-turnover experiments were in contrast with previous observations from the catalytic oxidation of Ac-Gly-NHtBu, which contained excess amounts of the oxidant $KHSO_5$ (Figure 10b). In this case, treatment of Ac-Gly-NHtBu with a catalytic amount (1 mol %) of $[Fe^{II}(N4Py)(CH_3CN)](ClO_4)_2$ and 5 equiv of $KHSO_5$ in a mixture of H_2O/CH_3CN (5:1) resulted in scission of the substrate and produced a mixture of **10** and **6** in 41% and 11% yields, respectively, along with 17% recovered starting material. Hemiaminal **5** (5%) and glyoxamide **7** (5%) were determined to be minor byproducts. The cleavage product **10** is consistent with alkoxyl radical intermediates,[6,68,69] and a divergent pathway for Gly oxidation is proposed. In this case, the radical chain process is proposed to be carried by $KHSO_5$, because the same cleavage products are observed under anaerobic conditions in the absence of O_2. The extent to which pathway A is followed relative to pathway B is not clear, because the hydroxylated product **5** could result from either pathway, in the case of autoxidation (pathway B), from the reaction of **9** with an H-atom donor.

Unreactive Amino Acids. Basic Amino Acids. Substrates derived from the basic amino acids Lys, Arg, and His did not react rapidly with the ferryl complex $[Fe^{IV}(O)(N4Py)]^{2+}$. In the case of Lys, rapid decomposition of $[Fe^{IV}(O)(N4Py)]^{2+}$ was observed ($t_{1/2} < 4$ min) when the free base Ac-Lys-NHtBu was added. However, because the reaction under pseudo-first-order conditions required an excess of substrate (10 equiv), the apparent pH of the solution was >9, so the decomposition could have been caused by the reaction of $[Fe^{IV}(O)(N4Py)]^{2+}$ with the amino side chain of Lys, or alternatively by the basic reaction medium.[45] No oxidation products of Ac-Lys-NHtBu were detected by NMR or ESMS analysis of the crude reaction mixture, consistent with high pH, leading to decomposition of the ferryl.[45] The addition of dilute aqueous NaOH (pH = 9) caused rapid decomposition of the ferryl, again consistent with the basic medium causing decomposition. The dependence on pH was confirmed when 1 equiv of HCl (relative to Ac-Lys-NHtBu)

(67) Eklund, H.; Fontecave, M. *Structure* **1999**, *7*, R257–R262.
(68) Wood, G. P. F.; Easton, C. J.; Rauk, A.; Davies, M. J.; Radom, L. *J. Phys. Chem. A* **2006**, *110*, 10316–10323.
(69) Davies, M. J. *Arch. Biochem. Biophys.* **1996**, *336*, 163–172.

was added prior to the addition of the ferryl species. In this case, the rate of decomposition slowed dramatically, with $k_{obs} = 1.4(2) \times 10^{-5}$ s^{-1} (see Table 1). These results are in direct contrast with the high reactivity of Lys toward ROS such as HO· and may suggest that reactivity of ferryl complexes with Lys residues in proteins would be slow at physiological pH, where these amino side chains would be protonated. Furthermore, the lack of reactivity demonstrated herein compared with anilines described previously[51] indicates that the free base of the amine is required to participate in the ET-PT mechanism for the reaction of amines with ferryl complexes. In the case of ammonium salts, ET from the amine to the $[Fe^{IV}(O)(N4Py)]^{2+}$ would be expected to be slow. Although the substrate derived from His was roughly 3-fold more reactive than Ac-Lys-NHtBu·HCl, this acceleration may be due to a pH effect, because no products derived from the His substrate were observed in the reaction with $[Fe^{IV}(O)(N4Py)]^{2+}$ under single-turnover conditions. Likewise, the substrate Ac-Arg-NHtBu·HCl was not reactive toward the ferryl species.

Polar Amino Acids. Decomposition rates for substrates derived from Ser and Thr that contained alcohol functional groups were 6.6 and 2.8 times faster than the control reaction with no substrate added, indicating that these amino acids were not highly reactive with the ferryl species $[Fe^{IV}(O)(N4Py)]^{2+}$ under the reaction conditions employed (298 ± 2 K, pseudo-first-order with 10 equiv of substrate). No products were detected in either case by ^{1}H NMR spectroscopy and ESMS analysis of the crude reaction mixtures. The slightly higher reactivity of Ser compared with Thr suggests that steric encumberance is more important than C−H bond strength in controlling reactivity, because the C−H bond adjacent to the alcohol group in the Thr substrate would be expected to be weaker than that contained on the primary alcohol of the Ser substrate on the basis of first principles. Substrates derived from Asp, Gln, Asn, and Glu showed decomposition rates for $[Fe^{IV}(O)(N4Py)]^{2+}$ that were identical within error, causing the ferryl to decompose only slightly faster than the control experiment with no substrate added. No oxidation products were identified under single-turnover conditions or under catalytic conditions with stoichiometric $KHSO_5$ as the oxidant.

Aliphatic Amino Acids. Substrates derived from the aliphatic amino acids Ala, Val, Leu, Ile, and Pro do not cause rapid decomposition of the ferryl $[Fe^{IV}(O)(N4Py)]^{2+}$ under the conditions shown in Table 1. These results indicate that abstraction of the α-H atom with substituted amino acids (e.g., R = Me; Figure 11) is slow compared with that of the Gly substrate (R = H). This observation was surprising, considering the fact that the bond dissociation energies of most α-hydrogens found in amino acid residues in proteins have been calculated to lie between approximately 80 and 90 kcal/mol,[70,71] dependent on the environment that the residue resides in (e.g., α-helix or *β*-sheet), but well below that of the reactivity limit of $[Fe^{IV}(O)(N4Py)]^{2+}$ (99 kcal/mol for C−H bond of cyclohexane).[37] A trend similar to the reactivity shown

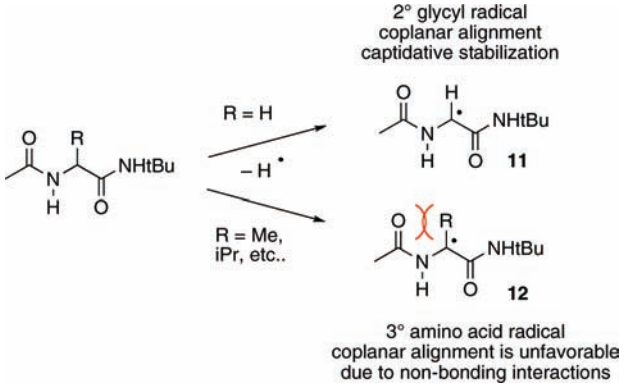

Figure 11. Carbon-centered radicals resulting from the abstraction of an α-hydrogen atom, stabilized in the case of Gly but destabilized with other amino acids.

in Table 1 was noted in the H-atom abstractions of *N*-benzoyl-amino acid esters with the bromine radical.[72] In this case, reactivity of the substrate derived from Gly was 3 times that of Ala (note similarity to data in Table 1) and over 20 times that of Val. This difference in reactivity stemmed from the ability of glycyl radicals to undergo captodative stabilization, which is likely to be operating herein as well (Figure 11). In order to achieve resonance stabilization, coplanar alignment of six contiguous sp^2-hybridized atoms is required for maximization of the orbital overlap, as shown in **11**, Figure 11. In the case of substituted amino acids such as Ala, a nonbonding interaction between the amide carbonyl and side chain (R) destabilizes this coplanar conformation, resulting in radical **12**, which does not enjoy the full energetic benefit of captodative stabilization. In addition to the α position being unreactive, activation of C−H bonds in the side chains of Val, Ile, and Leu, as well as the pyrrolidine ring of Pro, was not observed. These results prove that the secondary or tertiary C−H bonds located in the side chains of these amino acids are not reactive with $[Fe^{IV}(O)(N4Py)]^{2+}$ and may indicate that the kinetic reactivity of the ferryl can be attenuated by steric hindrance, because these bonds should be sufficiently weak to undergo activation (91−95 kcal/mol), albeit at a slow rate.[73] However, it should be noted that decomposition of the ferryl would likely be accelerated with higher concentrations of these substrates, where the rate of reaction with the substrate could out-compete the background rate of ferryl decomposition. Unfortunately, such studies with the aliphatic peptide models were not possible, due to the limited solubility of these compounds in the H_2O/CH_3CN solvent.

Conclusion

In conclusion, the reactivity of the ferryl species $[Fe^{IV}(O)(N4Py)]^{2+}$ with 20 natural amino acid substrates has been characterized. These studies are significant, because this is the first time that the reactivity of a well-characterized metal-based oxidant has been defined with all 20 amino acids. The

(70) Rauk, A.; Armstrong, D. A. *J. Am. Chem. Soc.* **2000**, *122*, 4185–4192.
(71) Rauk, A.; Yu, D.; Taylor, J.; Shustov, G. V.; Block, D. A.; Armstrong, D. A. *Biochemistry* **1999**, *38*, 9089–9096.
(72) Burgess, V. A.; Easton, C. J.; Hay, M. P. *J. Am. Chem. Soc.* **1989**, *111*, 1047–1052.
(73) McMillen, D. F.; Golden, D. M. *Annu. Rev. Phys. Chem.* **1982**, *33*, 493–532.

five most reactive amino acids, in order of decreasing reactivity, were Cys, Tyr, Trp, Met, and Gly. This study proves that $[Fe^{IV}(O)(N4Py)]^{2+}$ is a selective oxidant, unlike ·OH, which reacts with all amino acids with little variation in rate between the most and least reactive substrates.[4] Thiol-, phenol-, indole-, and sulfur-containing side chains are all highly reactive with the ferryl species, whereas amines (as ammonium salts), carboxylic acids, amides, guanidinium groups, benzyl groups, and alkyl chains are not susceptible to fast oxidation by $[Fe^{IV}(O)(N4Py)]^{2+}$. Mechanistic studies have revealed that the oxidation of Cys, Tyr, Trp, and Gly by $[Fe^{IV}(O)(N4Py)]^{2+}$ involves the loss of a hydrogen atom, either through ET-PT or HAT, whereas the mechanism for oxidation of Met involves O-atom transfer. The α position of amino acids is only susceptible to oxidation in the case of Gly, presumably due to the ability of the glycyl radical to undergo captodative stabilization, whereas amino acids with side chains other than H are not oxidized at this position.

The broad variation in rate constants observed in Table 1 suggests that $[Fe^{IV}(O)(N4Py)]^{2+}$ and other ferryls have the potential to oxidize proteins and other complex organic structures with high selectivity. The fact that side-chain oxidation is significantly faster than attack of the backbone at Gly suggests that the cleavage of proteins by ferryl complexes may be slow compared with side chain oxidation. That being stated, cleavage of the backbone is not required to achieve protein inactivation, as recently demonstrated by a copper-based metallopeptide.[74] Therefore, ferryl complexes have the potential to be useful reagents for protein inactivation. These studies are now underway in our laboratory.

Experimental Section

General Considerations. All reagents were purchased from commercial suppliers and used as received. NMR spectra were recorded on a Varian FT-NMR Unity-300, Mercury-400, or Oxford-500 MHz spectrometer. Mass spectra were recorded on a Waters ZQ2000 single quadrupole mass spectrometer using an electrospray ionization source. IR spectra were recorded on a Nicolet FT-IR spectrophotometer. High-performance liquid chromatography was performed on an Agilent 1200 Preparative Purification System equipped with a multiwavelength detector. UV−vis spectra were recorded on a Varian Cary 50 spectrophotometer. EPR spectra were recorded on a Bruker ESP 300 X-Band EPR spectrometer. Stopped-flow data were recorded on a Chirascan Circular Dichroism Spectrophotometer equipped with a KSHU stopped-flow apparatus. The complex $[Fe^{II}(N4Py)(CH_3CN)](ClO_4)_2$, used in this study, was synthesized according to a literature procedure.[75] The syntheses of substrates for these studies, of the general formula Ac-AA-NHtBu, where AA = amino acid, are described elsewhere.[76] An experimental procedure and characterization data for the oxidation products of Ac-Gly-NHtBu obtained under catalytic conditions were described previously.[59] Reactions were performed under ambient atmosphere unless otherwise noted.

General Procedure for Kinetic Experiments. Reactions of the species $[Fe^{IV}(O)(N4Py)]^{2+}$ with amino acid substrates were conducted at 298 ± 2 K under pseudo-first-order conditions. Rate constants represent the average of at least three runs. The reactions were monitored using a UV−vis spectrophotometer and were performed using the following standard procedure. A 2 mM solution of $[Fe^{II}(N4Py)(MeCN)](ClO_4)_2$ in 3:1 H_2O/MeCN (1.0 mL, 2 μmol) was treated with a solution of 1 equiv of oxone in H_2O (100 μL, 2 μmol). The solution was allowed to stand for 10 min, during which a color change from orange-red to green was noted. After 10 min, the $[Fe^{IV}(O)(N4Py)]^{2+}$ species was fully generated, as judged by maximization of the absorbance at 680 nm. The green solution of $[Fe^{IV}(O)(N4Py)]^{2+}$ was treated with a 10 equiv solution of the amino acid substrate in 1:3 H_2O/MeCN (900 μL, 20 μmol). After mixing (less than 10 s), the reaction was monitored by UV−vis spectroscopy. The absorbance traces for the decomposition of $[Fe^{IV}(O)(N4Py)]^{2+}$ (λ = 680 nm) showed first-order decay and fit well to the single exponential equation $[A = \Delta A(1 - e^{kt}) + A_0)]$ for substrates (Figures S2−S23, Supporting Information). Studies to determine KIE were conducted in the same manner as above except using the deuterated solvents CD_3CN and D_2O. Due to the fast reaction rates of highly reactive substrates, Ac-Cys-NHtBu and Ac-Tyr-NHtBu, which cause the decomposition of $[Fe^{IV}(O)(N4Py)]^{2+}$ within a few seconds, a stopped-flow apparatus was employed. The procedure follows that of the general procedure for kinetic experiments, except that the two solutions were loaded separately in syringes and were mixed using a KSHU stopped-flow apparatus. A Chirascan circular dichroism spectrophotometer was used to measure the absorbance at a single wavelength, 680 nm. Studies to determine KIE using stopped-flow conditions were conducted in the same manner as above except using the deuterated solvents CD_3CN and D_2O.

EPR Studies. EPR spectra were collected on a Bruker X-Band EPR spectrometer. See the figures for experimental conditions. Samples were prepared according to the aforementioned general procedure for kinetic studies, except that the solutions of $[Fe^{IV}(O)(N4Py)]^{2+}$ and the amino acid substrates were cooled to 0 °C before mixing and were freeze-quenched in liquid N_2.

3,3′-Disulfanediylbis(2-acetamido-*N*-*tert*-butylpropanamide) (1). A 2 mM solution of $[Fe^{II}(N4Py)(MeCN)](ClO_4)_2$ (1 mL, 2 μmol) in CH_3CN was stirred with 2 equiv of PhIO for 70 min to generate the ferryl species, $[Fe^{IV}(O)(N4Py)]^{2+}$. The excess PhIO was removed by filtration. A solution of Ac-Cys-NHtBu (1 mL, 20 μmol) in water (plus a few drops of acetonitrile for solubility) was added to the ferryl solution. After 14 h, the solution was concentrated in vacuo and dissolved in CD_3CN. To this solution, cyclooctadiene in CD_3CN (50 μL, 2 μmol) was added as an internal standard. By ^1H NMR analysis, the integrations of the singlet at 5.55 ppm, for the internal standard, and the multiplet at 4.96 ppm, for the cysteine disulfide, were used to calculate a 61% yield.

A different procedure was used to prepare **1** on a preparative scale. NaI (1.0 mg, 1.5 μmol) was added to a solution of *N*-Ac-Cys-NHtBu (33.0 mg, 151 μmol) in EtOAc (2 mL). H_2O_2 (14.8 μL, 151 μmol) was added, and the yellow mixture was allowed to stir for 3.5 h. A saturated solution of $Na_2S_2O_3$ (5 mL) was added upon completion of the reaction, as noted by thin-layer chromatography (TLC), and the crude product was extracted with EtOAc (2 × 5 mL). The organic layer was washed with brine (1 × 1 mL), dried over anhydrous sodium sulfate, and concentrated in vacuo. The residue was dissolved in EtOAc and passed through silica gel; the eluted solution was concentrated in vacuo to yield the disulfide of *N*-Ac-Cys-NHtBu (32 mg, quantitative). mp = 238−240 °C. ^1H NMR (CD_3OD): δ 4.66 (m, 2H), 3.05 (dd, J = 13.8 Hz, 8.9 Hz, 2H), 2.88 (dd, J = 13.8 Hz, 6.5 Hz, 2H), 1.98 (s, 6H), 1.33 (s, 18H). ^{13}C NMR (CD_3OD): δ 173.1, 171.4, 54.5, 52.4, 42.6, 28.8, 22.5. IR (KBr): 3726, 3628, 3290, 3081, 2967, 1645, 1557, 1455, 1393, 1365, 1263, 1225, 1176, 756, 668 cm^{-1}. LRMS (ESMS) calcd for $C_{18}H_{35}N_4O_4S_2$ $(M+H)^+$: 435. Found: 435.

2-Acetamido-*N*-*tert*-butyl-4-(methylsulfinyl)butanamide (2). $[Fe^{II}(N4Py)(MeCN)]$ $(ClO_4)_2$ (53.4 mg, 80.0 μmol) was

(74) Gokhale, N. H.; Bradford, S.; Cowan, J. A. *J. Am. Chem. Soc.* **2008**, *130*, 2388–2389.
(75) Roelfes, G.; Lubben, M.; W.; Leppard, S.; Schudde, E. P.; Hermant, R. M.; Hage, R.; Wilkinson, E. C.; Que, L., Jr.; Feringa, B. L. *J. Mol. Catal. A: Chem.* **1997**, *117*, 223–227.
(76) Ekkati, A. R.; Campanali, A. A.; Abouelatta, A. I.; Shamoun, M.; Kalapugama, S.; Kelley, M.; Kodanko, J. J. *Amino Acids* **2009**, in press.

dissolved in MeCN (40 mL) and stirred with PhIO (35.4 mg, 160 μmol) for 1 h, resulting in a green-colored solution of $[Fe^{IV}(O)(N4Py)](ClO_4)_2$ (2 mM). This solution was added to a solution of Ac-Met-NHtBu (20 mg, 80 μmol) in H_2O (40 mL) and stirred for 1 h. The solution turned from the original green color to an orange-yellow color, indicating the decomposition of $[Fe^{IV}(O)(N4Py)]^{2+}$. Solvent was removed in vacuo; the residue was dissolved in MeOH (5 mL) and passed through ion-exchange resin (Dowex 50wx4; 100 mesh), which was preactivated with 0.1 M HCl. The ligand, N4Py, as well as its Fe^{II} complex adhered to the column. The methanolic solution of the oxidation product of *N*-Ac-Met-NHtBu was concentrated in vacuo to yield a yellowish white solid (17 mg, 85%). ^{1}H NMR revealed a mixture of 1.7:1 starting material (54%) to sulfoxide derivative (31%).

A different procedure was used to prepare **2** on a preparative scale. A solution of Ac-Met-NHtBu (40 mg, 162 μmol) in 1:1 H_2O/CH_3CN was treated with oxone (50 mg, 81 μmol). After 90 s, the reaction was quenched by the addition of $Na_2S_2O_3$ (22 mg, 162 μmol). The reaction mixture was concentrated to remove CH_3CN, and the aqueous layer was extracted with CH_2Cl_2 (3×1 mL). The organic layer was dried over anhydrous sodium sulfate and concentrated in vacuo. The product was purified by silica gel chromatography (gradient; 1−10% $MeOH/CH_2Cl_2$), to yield **2** (15 mg, 35%) as mixture of sulfoxide diastereomers as a colorless liquid. ^{1}H and ^{13}C NMR spectra were complicated due to the presence of two diastereomers; only key peaks are reported. ^{1}H NMR ($CDCl_3$): δ 7.03 (m, 1H), 6.85 (m, 2H), 6.7 (s, 1H), 4.55 (m, 2H), 2.84 (m, 4H), 2.68 (s, 3H), 2.62 (s, 3H), 2.36 (m, 1H), 2.18 (m, 3H), 2.05 (s, 6H), 1.36 (s, 18H). ^{13}C NMR ($CDCl_3$): δ 170.8, 169.8, 52.0, 50.6, 49.2, 38.8, 37.6, 28.9, 27.6, 26.7, 23.4. IR ($CHCl_3$): 3290, 2966, 2925, 1650, 1549, 1451, 1430, 1392, 1365, 1259, 1226, 1032, 667 cm^{-1}. LRMS (ESMS) calcd for $C_{11}H_{23}N_2O_3S$ $(M+H)^+$: 263. Found: 263.

2-Acetamido-N-*tert*-butyl-3-(4-methoxyphenyl)propanamide. Iodomethane (70 μL, 0.97 mmol) was added to a yellow mixture of Ac-Tyr-NHtBu (220 mg, 790 μmol), K_2CO_3 (220 mg, 1.50 mmol), and DMF (40 mL); disappearance of the yellow color was observed during the progress of the reaction. The reaction progress was monitored by TLC, and upon completion, the mixture was concentrated in vacuo. The residue was dissolved in chloroform (20 mL) and ammonium chloride (20 mL). The organic layer was separated, and the aqueous layer was extracted with chloroform (4 × 20 mL). The combined organic layer was washed with water (1 × 10 mL), dried over anhydrous sodium sulfate, and concentrated in vacuo. Crude product was purified by silica gel flash column chromatography (gradient; 2−5% $MeOH/CH_2Cl_2$), yielding Ac-Tyr(OCH_3)-NHtBu (0.24 g, quantitative). mp = 225−227 °C. ^{1}H NMR (DMSO-d_6): δ 7.90 (d, J = 8.5 Hz, 1H), 7.47 (s, 1H), 7.12 (d, J = 8.24 Hz, 2H), 6.79 (d, J = 8.2 Hz, 2H), 4.39 (m, 1H), 3.69 (s, 3H), 2.78 (dd, J = 14.0 Hz, 5.5 Hz, 1H), 2.64 (dd, J = 13.4 Hz, 9.2 Hz, 1H), 1.74 (s, 3H), 1.19 (s, 9H). ^{13}C NMR (DMSO-d_6): δ 170.6, 168.8, 157.7, 130.2, 129.8, 113.3, 54.9, 54.3, 50.0, 37.5, 28.4, 22.5. IR (KBr): 3268, 3082, 2965, 2826, 1637, 1559, 1515, 1451, 1391, 1363, 1289, 1252, 1227, 1178, 1041 cm^{-1}. LRMS (ESMS) calcd for $C_{16}H_{25}N_2O_3$ $(M+H)^+$: 293. Found: 293.

4-(2-Acetamido-3-(*tert*-butylamino)-3-oxopropyl)phenyl Acetate. Acetic anhydride (350 μL, 3.59 mmol) was added to a mixture of Ac-Tyr-NHtBu (500 mg, 1.79 mmol), triethylamine (750 μL, 5.45 mmol), and DMF (10 mL) at 0 °C under an inert atmosphere. The reaction mixture was warmed to room temperature, stirred for 12 h, and was concentrated in vacuo. The residue was dissolved in EtOAc (10 mL), and the organic layer was washed with ammonium chloride (3 × 10 mL), sodium bicarbonate (3 × 10 mL), and brine (3 × 10 mL). The organic layer was dried over anhydrous sodium sulfate and concentrated in vacuo. The product was collected by vacuum filtration after stirring with ether (2 mL). The solid was dissolved in CH_2Cl_2 (3 × 10 mL) and concentrated in vacuo to yield Ac-Tyr-(OAc)-NHtBu (0.55 g, quantitative). mp = 225−227 °C. ^{1}H NMR (DMSO-d_6): δ 8.03 (d, J = 8.9 Hz, 1H), 7.52 (s, 1H), 7.24 (d, J = 8.0 Hz, 2H), 6.98 (d, J = 8.1 Hz, 2H), 4.44 (m, 1H), 2.84 (dd, J = 13.8 Hz, 5.7 Hz 1H), 2.73 (dd, J = 12.4 Hz, 8.9 Hz 1H), 2.29 (s, 3H), 1.75 (s, 3H), 1.18 (s, 9H). ^{13}C NMR (DMSO-d_6): δ 170.4, 169.2, 168.9, 148.9, 135.4, 130.2, 121.2, 54.1, 50.1, 37.6, 28.4, 22.5, 20.9. IR (KBr): 3282, 3074, 2967, 2917, 1765, 1643, 1555, 1508, 1451, 1366, 1216, 1196, 1166, 1018, 911 cm^{-1}. LRMS (ESMS) calcd for $C_{17}H_{25}N_2O_4$ $(M+H)^+$: 321. Found: 321.

Acknowledgment. We thank Dr. Andrew Feig and Dr. David Rueda for assistance with stopped-flow studies, Marco Allard for assistance with EPR spectroscopy, Danielle Zurcher for the synthesis of amino acid substrates, and Wayne State University for its generous support of this research.

Supporting Information Available: UV−vis, EPR, and NMR spectra and kinetic fits. This material is available free of charge via the Internet at http://pubs.acs.org.